ACES Asian Chemical Editorial Society

doi.org/10.1002/asia.202400824

CHEMISTRY
AN ASIAN JOURNAL
Research Article

www.chemasianj.org

Selective Protein Degradation through Tetrazine Ligation of Genetically Incorporated Unnatural Amino Acids

Jinghao Chen,[a, b] Gaocan Dai,[b] Shixiang Duan,[b] Yang Huang,[b, c] Yi-Lin Wu,*[d] Zhiyong Xie,*[a] and Yu-Hsuan Tsai*[b]

Small molecule-responsive tags for targeted protein degradation are valuable tools for fundamental research and drug target validation. Here, we show that genetically incorporated unnatural amino acids bearing a strained alkene or alkyne functionality can act as a minimalist tag for targeted protein degradation. Specifically, we observed the degradation of strained alkene- or alkyne-containing kinases and E2 ubiquitin-conjugating enzymes upon treatment with hydrophobic tetrazine conjugates. The extent of the induced protein degradation depends on the identity of the target protein, unnatural amino acid, and tetrazine conjugate, as well as the site of the unnatural amino acid in the target protein. Mechanistic studies revealed proteins undergo proteasomal degradation after tetrazine tethering, and the identity of tetrazine conjugates influences the dependence of ubiquitination on protein degradation. This work provides an alternative approach for targeted protein degradation and mechanistic insight, facilitating the future development of more effective targeted protein degradation strategies.

Introduction

Proteins are the workhorse molecules, playing critical roles for all living organisms. Approaches for selective protein degradation are powerful methods for determining protein function and understanding complex biological systems.[1] Here, the biological outcome is similar to genetic knockout of the corresponding DNA or knockdown of the corresponding mRNA. Nevertheless, directly targeting the protein of interest for degradation acts much more rapidly than targeting its predecessor nucleic acids.

To date, many bi-functional small molecules have been developed for targeted protein degradation.[2] In some cases, these small molecules (also known as proteolysis-targeting chimera, PROTAC) bind to the target protein and an E3 ubiquitin ligase, leading to polyubiquitination of the target protein and its proteasomal degradation. Alternatively, the small molecules can simultaneously bind to the target protein and a key protein for lysosomal trafficking, leading to lysosomal degradation of the target protein. Notably, these approaches rely on the availability of selective small-molecule ligands, which are not available for many proteins.[3]

Small molecule-responsive protein tags eliminate the need for target-specific ligands and are valuable biological tools[4] Here, a tag of around 40–300 amino acids is genetically fused to the target protein so that the addition of a small molecule induces degradation or stabilization of the target.[5] A recent comparative study of five degradation tags, AID,[5a] dTAG,[5e] HaloTag,[5d] IKZF3d,[5f] and SMASh,[5c] revealed that many factors influenced the extent of inducible degradation, and there was no best tag with highest performance across all tested targets.[6] Therefore, identifying new protein degradation tags with different mechanisms of action and minimal structural perturbation may provide valuable tools for fundamental research and drug target validation.

Here, we show that genetically encoded unnatural amino acids bearing a strained alkene or alkyne functionality can act as a minimalist tag for protein degradation induced by tetrazine conjugates. The unnatural amino acids undergo rapid inverse electron demand Diels-Alder reaction with tetrazines to afford adducts with increased hydrophobicity (Figure 1). Indeed, tagging hydrophobic molecules (e.g., adamantane,[7] Boc3Arg,[8] carborane,[9] fluorene,[10] norbornene,[11] pyrene,[12] etc.) to the target protein by small molecules or protein tags has been successfully applied to induce protein degradation.

Similar to other degradation tags,[6] we found that the performance of tetrazine-mediated degradation depended on many factors, including the identity of the protein target, tetrazine conjugate, and unnatural amino acid, as well as the incorporation site of unnatural amino acid. Generally, tethering of more hydrophobic tetrazine conjugates (i.e., adamantane or Boc3Arg) was more effective in inducing the degradation of

[a] J. Chen, Z. Xie
School of Pharmaceutical Sciences (Shenzhen), Sun Yat-Sen University, Shenzhen, China
E-mail: xiezhy@mail.sysu.edu.cn

[b] J. Chen, G. Dai, S. Duan, Y. Huang, Y.-H. Tsai
Institute of Molecular Physiology, Shenzhen Bay Laboratory, Shenzhen, China
E-mail: tsai.y-h@outlook.com

[c] Y. Huang
School of Basic Medical Sciences, Capital Medical University, Beijing, China

[d] Y.-L. Wu
School of Chemistry, Cardiff University, Cardiff, United Kingdom
E-mail: wuyl@cardiff.ac.uk

Supporting information for this article is available on the WWW under https://doi.org/10.1002/asia.202400824

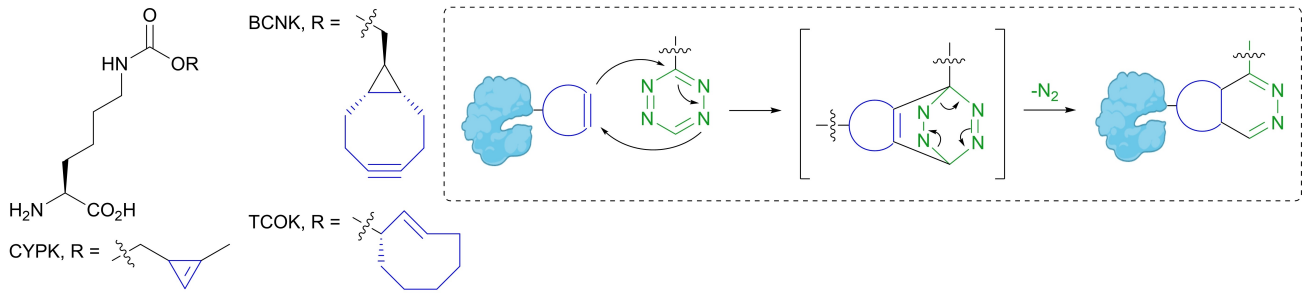

Figure 1. Structure of genetically incorporable unnatural amino acids BCNK, CYPK, and TCOK, which can undergo inverse electron demand Diels-Alder reaction with tetrazines.

PKA kinases and E2 ubiquitin-conjugating enzymes. Similarly, the bulkier unnatural amino acids bicyclo[6.1.0]non-4-yne lysine (BCNK) and *trans*-cyclooct-2-en lysine (TCOK) seemed to be better than cyclopropene lysine (CYPK). Mechanistic studies revealed proteasomal degradation of the target protein after tetrazine ligation, although the process was not dependent on either HSP70 or E3 ubiquitin ligase CHIP, in contrast to the literature.[7a–c]. In addition to hydrophobic motifs, genetically incorporated unnatural amino acids can also be used to tether molecules of diverse functionalities. Thus, they represent an alternative and minimalist tag for targeted protein degradation.

Results and Discussion

Inducible Degradation of Proteins after BCN-Mediated Tetrazine Ligation

Genetic code expansion enables site-specific introduction of an unnatural amino acid in response to the amber (UAG) codon into a ribosomal translated protein and is useful for introducing bioorthogonal functionality for protein modification.[13] For example, BCNK is a genetically incorporable unnatural amino acid that undergoes rapid inverse electron demand Diels-Alder reaction with tetrazines (Figure 1).[14] Previously, we incorporated BCNK into intracellular kinases for their functional regulation upon bioorthogonal tethering with tetrazine conjugates.[15] During our investigation of selective inhibition of cAMP-dependent protein kinase catalytic subunit alpha (PKA–Cα),[15b] we serendipitously found that the abundance of some BCNK-bearing PKA–Cα variants seemed to be affected by bioorthogonal tethering. For example, PKA–Cα with Ile135BCNK mutation, PKA–Cα(135BCNK), was one of such variants, of which the abundance decreased upon treatment with **1** (tetrazine conjugate derived from a known PKA inhibitor,[16] Figure 2a). The observed effect depended on tetrazine ligation, as **1** had no effect on wild-type PKA–Cα (Figure 2b).

We also observed a similar phenomenon while investigating the feasibility of selective inhibition of E2 activity by bioorthogonal tethering in live mammalian cells.[17] We found the abundance of UBE2L3(90BCNK) reduced after treatment with simple tetrazine conjugate **2** (Figure 2c). We envisaged such a reduction was due to protein degradation. Indeed, pretreatment of cells with proteasome inhibitor MG-132 or bortezomib abolished this reduction, while lysosome inhibitor leupeptin or bafilomycin A1 had no effects, indicating proteasomal degradation of the BCNK-containing variants upon tetrazine ligation (Figure 2b and c).

It has been reported that binding of a hydrophobic molecule to the target protein can induce protein degradation,[18] and the reaction of BCNK with tetrazine conjugate **1** or **2** affords a more hydrophobic adduct indicated by computational analysis. Calculated logarithm of the partition coefficient of a molecule between *n*-octanol and water (clogP) is commonly used as a surrogate for hydrophobicity, and clogP values increased upon tetrazine ligation (Figures S1 and S2; Table S1).[19] Although specific values vary between different algorithms, they all closely correlate with each other with pairwise Pearson correlation coefficients between 0.668 and 0.949 (Table S2). Specifically, reactions of BCNK with **1** or **2** led to increases of 3.3 and 2.3 units, respectively, calculated by ALogP algorithm, indicating about 2000- and 200-fold increases in partitions into the non-polar octanol in preference to the aqueous phase.

We thus envisaged that the tethering of the protein with a more hydrophobic motif could enhance protein degradation. To this end, we synthesized tetrazine conjugates **3** and **4** containing an adamantane and Boc3Arg, respectively, which are often employed in small-molecule hydrophobic tagging (HyT)-induced degradation.[18] Reaction of BCNK with **3** or **4** would afford adducts with higher clogP values than that of with **1** or **2** (Table S1). Experimentally, conjugates **3** and **4** were able to induce degradation of PKA–Cα(135BCNK) and UBE2L3(90BCNK), and pretreatment with proteasome inhibitors, but not lysosome inhibitors, prevented protein degradation of tethered proteins (Figure 2b and c), confirming that these tetrazine conjugates induced protein degradation via the proteasome pathway. It is noteworthy that a recent study showed an adamantane derivative mediated degradation of CDK4/6 kinases via both proteasome and lysosome pathways,[20] although tetrazine conjugate **1**–**4** did not seem to induce lysosomal degradation of BCNK-containing proteins.

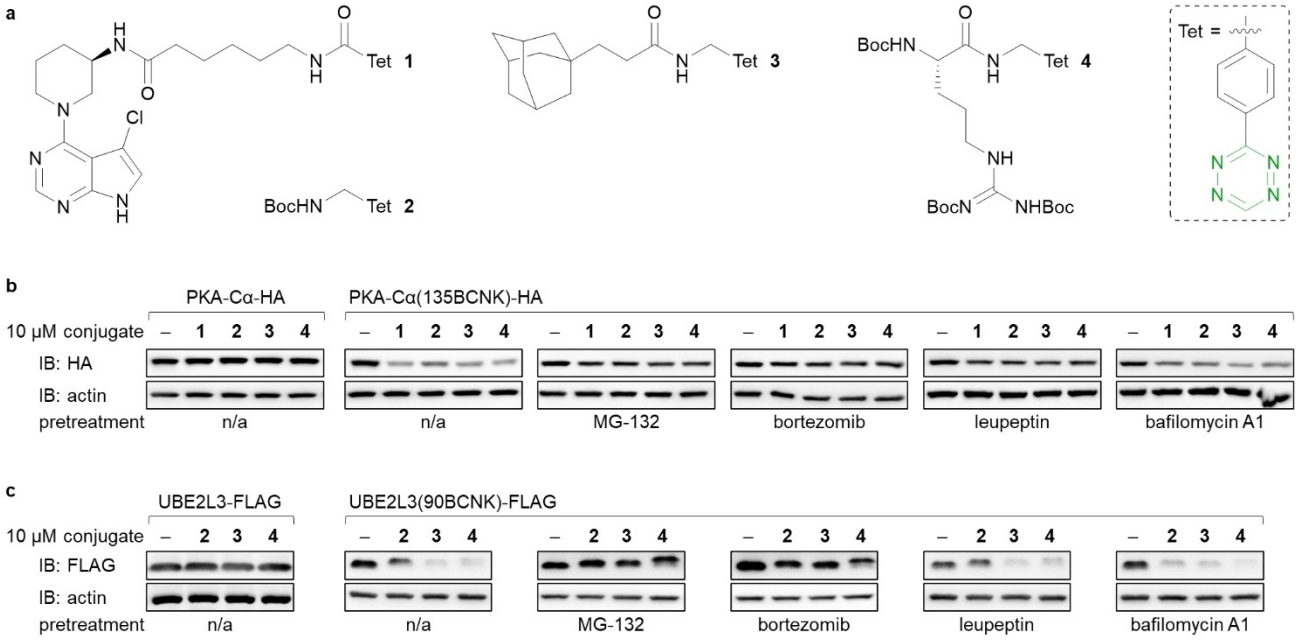

Figure 2. Immunoblotting of cellular PKA–Cα and UBE2L3 abundance after BCN-mediated bioorthogonal tethering. (a) Structure of tetrazine conjugates **1**–**4**. (b, c) Tetrazine conjugates induced proteasomal degradation of PKA–Cα(135BCNK)-HA and UBE2L3(90BCNK)-FLAG in HEK293T cells. HEK293T cells were transiently transfected with plasmids expressing a PylRS(AF)/tRNACUA for BCNK incorporation and a PKA–Cα or UBE2L3 variant. Codon of the amino acid residue designated for BCNK incorporation was changed to TAG to achieve amber suppression. Cells were cultured in the presence or absence of 0.1 mM BCNK for 48 h, followed by treatment with 10 μM of the indicated tetrazine conjugate for 2 h in the absence of BCNK. If required, cells were pretreated with the indicated inhibitor before addition of the tetrazine conjugate. Pretreatment conditions: 10 μM MG-132 for 2 h; 10 μM bortezomib for 1 h; 10 nM leupeptin for 2 h; 5 μM bafilomycin A1 for 2 h.

Effects of BCN Incorporation Site on Induced Protein Degradation

We next investigated the effect of the BCNK incorporation site on induced protein degradation. Since we did not notice such an effect previously during our investigation of kinases MEK1, MEK2, and LCK,[15a] and the degradation was more prominent in UBE2L3 than PKA–Cα (Figure 2), we chose another E2 ubiquitin-conjugating enzyme, UBE2L6, as the model protein. We randomly selected 15 solvent-exposed residues (Figure S3) for mutation to BCNK and found the abundance of most variants reduced upon tethering with tetrazine conjugate **2**, **3**, or **4** (Figures 3 and S4). Interestingly, after tetrazine conjugation, 91BCNK variant was stable, whereas 88/89/90/93/94BCNK variants diminished. While it is difficult to predict which variant would be responsive, identifying a responsive variant is relatively straightforward after screening a small library.

Generally, BCNK-containing UBE2L6 variants, of which degradation could be induced by Boc-protected tetrazine **2**, also responded to more hydrophobic adamantane conjugate **3** and Boc3Arg conjugate **4** (Figure 3). Even for variants less or not responsive to **2**, such as UBE2L6(69BCNK) and UBE2L6(84BCNK), degradation was observed upon treatment with more hydrophobic conjugate **3** or **4**, aligning with the computational analysis (Table S1) and literature reports of hydrophobic tagging for protein degradation.[7,8]

General Applicability of Tetrazine-Mediated Ligation for Protein Degradation

To evaluate the general applicability of BCNK-mediated tetrazine ligation for protein degradation, we incorporated BCNK into PKA–Cβ and other E2 enzymes, including UBE2B, UBE2C, UBE2D1, UBE2I, UBE2K and UBE2S. The stability of PKA–Cβ (Figure 4a) as well as UBE2B, UBE2C, UBE2D1 and UBE2S (Figure 4b) could be regulated by bioorthogonal tethering, indicating the general applicability of this phenomenon.

Apart from BCNK, cyclopropene lysine (CYPK) and *trans*-cyclooctene lysine (TCOK) can also undergo inverse electron demand Diels-Alder reactions with tetrazines, and their resulting adducts with tetrazine conjugates **1**–**4** also have higher clogP values than the corresponding amino acids (Table S1), consequently likely to induce protein degradation. To this end, we evaluated the stability of PKA–Cα and PKA–Cβ with residue 133 or 135 mutated to either CYPK, BCNK or TCOK upon tetrazine tethering, as well as UBE2L3 and UBE2L6 with residue 87, 89 or 90 mutated (Figure 5). In all combinations tested, degradation of CYPK-containing variants was generally less prominent, although clear degradation could also be observed in several cases, such as PKA–Cα(133CYPK) or UBE2L3(87CYPK) after treatment with **4**. On the other hand, degradation of TCOK-containing variants was much more prominent. As CYPK contains a three-membered ring, whereas both BCNK and TCOK contain an eight-membered aliphatic ring, the larger rings might impose greater hydrophobicity upon bioorthogonal tethering, consequently destabilizing the tethered proteins.

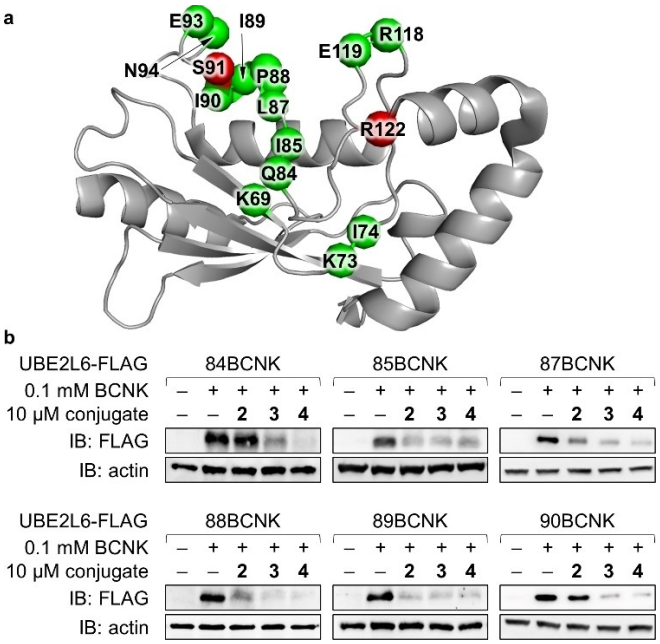

Figure 3. Immunoblotting of cellular abundance change of UBE2L6 incorporated with BCNK in different sites in response to tetrazine conjugates **2**–**4**. (a) Structure of UBE2L6 with BCNK incorporation site responsive (in green) and non-responsive (in red) to degradation induced by tetrazine conjugates (pdb: 1WZV). The enzyme contains a catalytic cysteine residue at position 86. See Figure S3 for the structure in surface and sidechain stick models. (b) Abundance of UBE2L6 variants with BCNK at position 84, 85, 87, 88, 89 or 90 under different conditions. HEK293T cells were transiently transfected with plasmids expressing a PylRS(AF)/tRNACUA for BCNK incorporation and a UBE2L6-FLAG variant. Codon of the amino acid residue designated for BCNK incorporation was changed to TAG to achieve amber suppression. Cells were cultured in the presence or absence of 0.1 mM BCNK for 48 h, followed by treatment with 10 μM of the indicated tetrazine conjugate for 2 h in the absence of BCNK. For cells cultured in the absence of BCNK, no protein was detected, demonstrating the specificity of BCNK incorporation. Results of variants with BCNK at positions 69, 73, 74, 91, 93, 94, 118, 119 or 122 are shown in Figure S4.

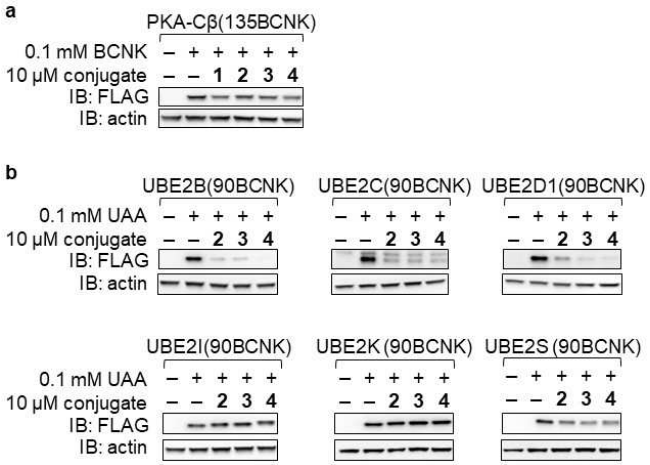

Figure 4. Immunoblotting of cellular abundance change of PKA–Cβ (a) and E2 ubiquitin-conjugating enzymes (b) bearing BCNK in response to tetrazine conjugates **2**–**4**. HEK293T cells were transiently transfected with plasmids expressing a PylRS(AF)/tRNACUA for BCNK incorporation and a PKA–Cβ or E2 variant. Codon of the amino acid residue designated for BCNK incorporation was changed to TAG to achieve amber suppression. Numbering of PKA–Cβ and E2 enzymes follows the numbering of PKA–Cα and UBE2L3, respectively. Cells were cultured in the presence or absence of 0.1 mM BCNK for 48 h, followed by treatment with 10 μM of the indicated tetrazine conjugate for 2 h in the absence of BCNK.

Overall, the extent of protein degradation depended on the site of tethering, choice of the unnatural amino acids (i.e., CYPK, BCNK or TCOK) and structure of the tetrazine conjugate. In addition, the observed phenomenon was not always transferable between protein homologues. For example, the abundance of UBE2L6(89BCNK) decreased after treatment with any of the three tested tetrazine conjugates, whereas the abundance of UBE2L3(89BCNK) showed negligible change. Nevertheless, identifying a set of parameters that could induce prominent degradation is rather straightforward, as protein degradation was observed in many of the tested combinations.

Mechanistic Investigation of Tetrazine-Mediated Ligation for Protein Degradation

A detailed understanding of the degradation mechanisms is essential for developing new targeted protein degradation strategies. While some studies shine light on the degradation pathways for hydrophobic tagging, the precise mechanism remains largely elusive.[18] Here, we used UBE2L6(89BCNK) as the model for investigating the degradation mechanism upon tethering with tetrazine conjugates **2**–**4**.

We first investigated the effect of the concentration of tetrazine conjugates on the abundance of UBE2L6(89BCNK).[21] Basically, a relatively low concentration of 0.3 μM was sufficient to trigger the degradation, and the extent of degradation remained largely unchanged between 1 and 30 μM tetrazine conjugates, consistent with the covalent tethering characteristics (Figure 6a). We then investigated the kinetics of degradation by conjugates **2**–**4**. Degradation by bioorthogonal tethering was expected to occur more slowly than conventional small molecule-triggered degradation, because the bioorthogonal tethering must take place first before proteasomal degradation of the tethered protein. Nevertheless, we observed clear degradation after one hour, which is faster than some hydrophobic tagging-based small molecules.[10,11,20,22]

It is generally believed that hydrophobic tagging mimics misfolded proteins, which are eliminated by the cellular quality control machinery.[18] Previous studies indicated that HSP70 is a chaperone recognizing adamantane-modified proteins, which is then likely ubiquitinated by the HSP70-associated E3 ubiquitin ligase CHIP before degradation by 26S proteasomes.[7a–c] Thus, we first used apoptozole (APZ) and geldanamycin to probe the involvement of HSP70 in tetrazine-mediated protein degradation. APZ is an inhibitor of HSP70,[23] whereas geldanamycin induces the expression of HSP70.[24] While treatment of geldanamycin led to an increase in the protein level of HSP70, neither APZ nor geldanamycin had a prominent effect on UBE2L6(90BCNK) degradation induced by tetrazine conjugates (Figure 6b). We also generated HSP70 or CHIP knockout (KO) HEK293T cells, in which degradation mediated by tetrazines, including adamantane derivative **3**, still occurred (Figure 6c).

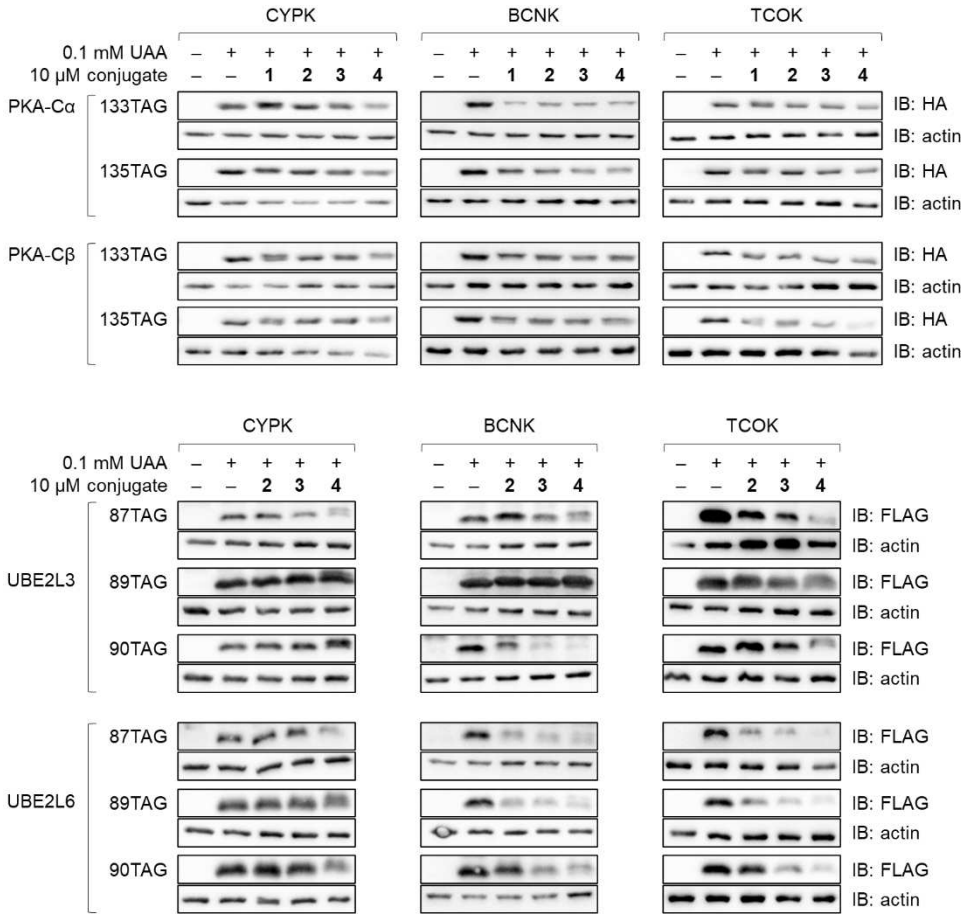

Figure 5. Effects of unnatural amino acid on protein degradation induced by tetrazine ligation. HEK293T cells were transiently transfected with plasmids expressing a PylRS/tRNACUA for CYPK incorporation or PylRS(AF)/tRNACUA for BCNK or TCOK incorporation, as well as a PKA or E2 variant. Codon of the amino acid residue designated for unnatural amino acid incorporation was changed to TAG to achieve amber suppression. Cells were cultured in the presence or absence of 0.1 mM unnatural amino acid for 48 h, followed by treatment with 10 μM of the indicated tetrazine conjugate for 2 h in the absence of unnatural amino acid.

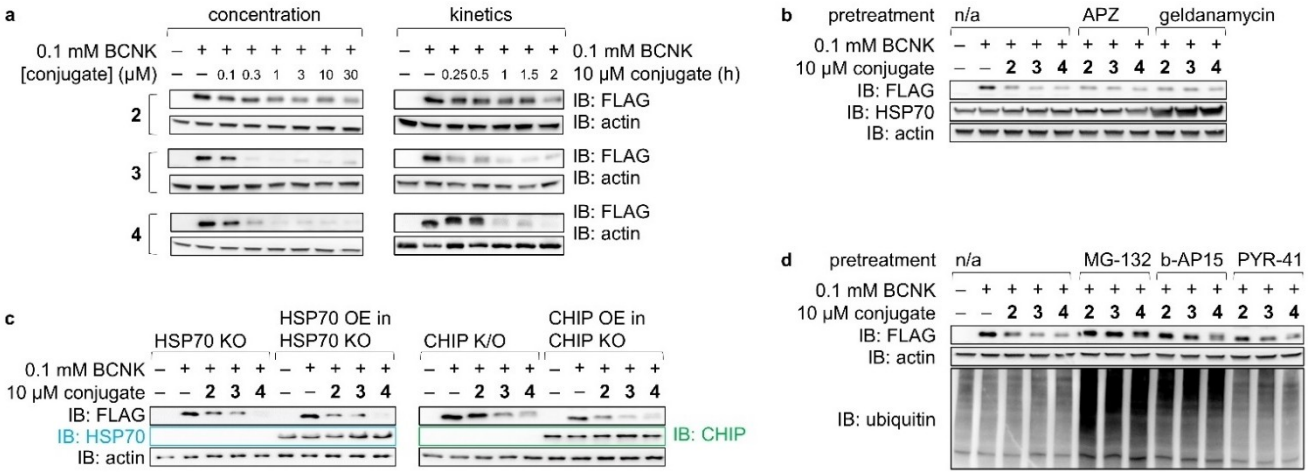

Figure 6. Mechanistic study with UBE2L6(89BCNK) as the model protein. (a) Effect of conjugate concentration and incubation time on protein degradation. (b) Effect of pharmacological HSP70 inhibition (apoptozole, APZ) or activation (geldanamycin) on protein degradation. (c) Effect of HSP70 or CHIP knockout on protein degradation. KO = knockout; OE = overexpression. (d) Effect of 20S proteasome inhibitor MG-132, 19S proteasome inhibitor b-AP15 and E1 ubiquitin-activating enzyme inhibitor PYR-41 on protein degradation. HEK293T cells were transiently transfected with plasmids expressing a PylRS(AF)/tRNACUA for BCNK incorporation and UBE2L6(90TAG)-FLAG. Cells were cultured in the presence or absence of 0.1 mM BCNK. For pharmacological treatment, cells were pretreated with 10 μM APZ for 16 h, 0.5 μM geldanamycin for 24 h, 10 μM MG-132 for 2 h, 1 μM b-AP15 for 2 h or 40 μM PYR-41 for 2 h before addition of the tetrazine conjugate. At the time point of conjugate addition, cells were cultured in the presence of 0.1 mM BCNK for 48 h. Unless otherwise stated, cells were incubated with 10 μM of the indicated tetrazine conjugate for 2 h.

Hence, the process was unlikely to depend on either HSP70 or CHIP, in contrast to the literature examples of degradation induced by adamantane tagging.[7a–c]

It is noteworthy that a recent report showed that norbornene-tagged proteins could undergo proteasomal degradation but did not bind to HSP70.[11] In addition, Boc3Arg was found to directly associate with 20S proteasome for ubiquitin-independent degradation of the tagged proteins.[8b] Thus, we proceeded to investigate the ubiquitin-dependency of tetrazine ligation-mediated degradation.

In eukaryotic cells, proteins are normally selected for degradation by undergoing covalent tagging with ubiquitin, typically through Lys48-linked chains. Subsequently, these ubiquitinated proteins undergo proteolysis within the 26S proteasome. The 26S proteasome is composed of a 19S regulatory particle and a 20S core particle. The 19S regulatory particle is primarily responsible for recognizing and removing ubiquitin from its client proteins, as well as unfolding them to facilitate their entry into the 20S core particle.[25] The 20S core particle is a barrel-shaped protein complex capable of hydrolyzing peptide bonds in a wide range of substrates,[26] generating various short peptide products. In addition, 20S can also function as a stand-alone proteasome to degrade target proteins in a ubiquitin-independent manner.[26,27]

MG-132 inhibits the proteolytic activity of 20S, so that it blocks the function of both 26S and 20S proteasomes. On the other hand, b-AP15 inhibits the deubiquitination by 19S regulatory particle, so that 26S proteasomes are unable to degrade ubiquitinated proteins. Lastly, PYR-41 is an E1 ubiquitin-activating enzyme inhibitor. Treatment of HEK293T cells with MG-132 or b-AP15, in contrast to PYR-41, led to an accumulation of ubiquitinated proteins as expected (Figure 6d). Specifically, pretreatment with b-AP15 seemed to prevent degradation induced by conjugates **2** and **3**. A similar phenomenon was observed for conjugate **2** in PYR-41 pretreated cells. These results indicated the involvement of protein ubiquitination in degradation induced by **2** and **3**, but not **4**. Nevertheless, the lower restoration in comparison to MG-132 treatment suggests the potential involvement of ubiquitin-independent degradation as well.

Conclusions

We show that genetically incorporated unnatural amino acids CYPK, BCNK, or TCOK can act as a minimalist tag for targeted protein degradation upon tethering with hydrophobic tetrazine conjugates. While the extent of the induced protein degradation depends on the identity of the target protein, hydrophobicity of the tetrazine conjugate, as well as structure and incorporation site of the unnatural amino acid, it is relatively straightforward to identify a combination leading to protein degradation, which could be an undesirable outcome for site-specific modification of cellular proteins through genetically incorporated unnatural amino acids.

Mechanistically, proteins tethered with Boc3Arg tetrazine conjugate **4** underwent ubiquitin-independent degradation by 20S proteasomes, whereas degradation of proteins tethered with Boc-protected tetrazine **2** or adamantane tetrazine **3** depended (at least in part) on ubiquitination. In all cases, degradation of proteins tethered with the tested tetrazine conjugates does not require HSP70. Thus, our results suggest the involvement of an alternative, yet unknown, mechanism for recognizing hydrophobic tagged proteins and mediating their ubiquitination.

Overall, our work provides an alternative approach for targeted protein degradation and mechanistic insight into degradation by hydrophobic tagging, facilitating the future development of more effective targeted protein degradation strategies.

Experimental Section

Estimation of the Lipophilicity Change After Tetrazine Ligation

Predicted values of the logarithm of octanol-water partition coefficients (logP), as a measure of lipophilicity, were calculated using established atom- or fragment-based empirical algorithms[19d] or through quantum chemical methods. In the latter approach, initial molecular geometry optimization was conducted using the MMFF94 s force field in Avogadro,[19c] followed by further optimization employing Grimme's low-cost B97-3c DFT method. The difference in solvation free energy between water and octanol was subsequently evaluated at the level of ωB97M–V/def2-TZVP with SMD implicit solvation, using ORCA 5.0.[19a,b] The resulting logP values were determined according to the equation: $\log P = [(\Delta G_{water} - \Delta G_{octanol})/(2.303RT)]$, where R and T are the molar gas constant and temperature, respectively, and $\Delta G_{solvent}$ is solvation free energy. For empirical estimations, molecular structures in various formats: ChemDraw structures (for BioByte ClogP), geometry-optimized 3-dimensional structures in the SYBYL MOL2 format (for XLOGP3,[19f] ALOGPS,[19e] and OBLogP), or SMILES strings generated from MOL2 files by OpenBabel (for AlogP)[19g] were used as inputs for the respective software.

Chemical Synthesis of Tetrazine Conjugates

Tetrazine conjugate **2** was prepared according to the literature procedure.[28]

Synthesis of 1

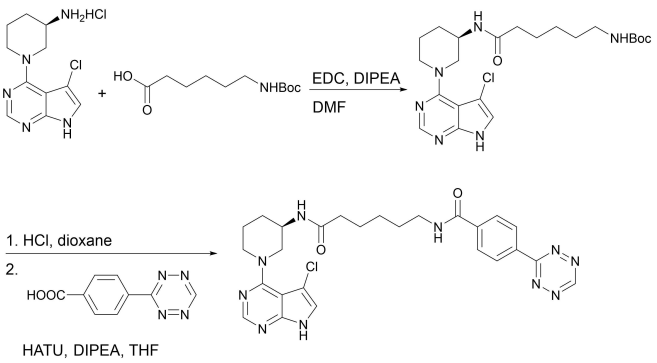

To a solution of *N*-Boc-6-aminocaproic acid (51 mg, 0.22 mmol, 1.1 equiv.) in DMF (2 mL) was added DIPEA (52 μL, 0.30 mmol, 1.5 equiv.) and EDC (53 μL, 0.30 mmol, 1.5 equiv.), followed by addition of (*R*)-1-(5-chloro-7*H*-pyrrolo[2,3-*d*]pyrimidin-4-yl)piperidin-3-amine hydrochloride (58 mg, 0.20 mmol, 1.0 equiv.).[16] After 12 h, EtOAc (50 mL) was added. The reaction mixture was washed with $NaHCO_{3(aq)}$ (50 mL×2) and brine (50 mL), dried over Na_2SO_4, filtered, and concentrated. The residue was purified by silica gel flash column chromatography (2% MeOH in DCM) to afford *tert*-butyl (*R*)-(6-((1-(5-chloro-7*H*-pyrrolo[2,3-*d*]pyrimidin-4-yl)piperidin-4-yl)piperi-din-3-yl)amino)-6-oxohexyl)carbamate (40 mg, 0.09 mmol, 43%). ^{1}H NMR (400 MHz, $CDCl_3$) δ 11.17 (s, 1H), 8.35 (s, 1H), 7.16 (s, 1H), 6.77 (brs, 1H), 4.59 (s, 1H), 4.17 (s, 1H), 3.89–3.84 (m, 2H), 3.66–3.57 (m, 2H), 3.08 (q, *J* = 6.8 Hz, 2H), 2.17–2.13 (m, 2H), 1.87–1.79 (m, 2H), 1.62–1.55 (m, 2H), 1.48–1.45 (m, 1H), 1.43 (s, 9H), 1.34–1.24 (m, 3H). ^{13}C NMR (101 MHz, $CDCl_3$) δ 172.5, 160.0, 156.2, 151.4, 151.0, 140.06, 140.03, 120.1, 79.3, 52.5, 52.3, 46.0, 40.5, 37.0, 29.9, 29.28, 28.6, 26.5, 25.4, 22.3. ESI-(+)-HRMS $[M+H]^+$ calculated for $C_{22}H_{33}ClN_6O_3$: 465.2375; found, 465.2375.

For Boc removal, the *tert*-butyl (*R*)-(6-((1-(5-chloro-7*H*-pyrrolo[2,3-*d*]pyrimidin-4-yl)piperidin-4-yl)piperi-din-3-yl)amino)-6-oxohexyl)carbamate (19 mg, 0.04 mmol 1.2 equiv.) was treated with 4 N HCl in dioxane for 1 h at room temperature. The solvent was then removed under reduced pressure to afford the (*R*)-6-amino-*N*-(1-(5-chloro-7*H*-pyrrolo[2,3-*d*]pyrimidin-4-yl)piperidin-3-yl)hexanamide hydrochloride as a white solid. For conjugation, 4-(1,2,4,5-tetrazin-3-yl)benzoic acid (7 mg, 0.04 mmol, 1.0 equiv.)[28] was dissolved in a solution of DIPEA (12 μL, 0.07 mmol, 2.0 equiv.) in dry THF (2 mL). HATU (20.0 mg, 0.05 mmol, 1.5 equiv.) was added, and the reaction mixture was allowed to stir at room temperature for 2 h under argon before the addition of (*R*)-6-amino-*N*-(1-(5-chloro-7*H*-pyrrolo[2,3-*d*]pyrimidin-4-yl)piperidin-3-yl)hexanamide hydrochloride. After 4 h, the reaction mixture was concentrated under reduced pressure. The obtained residue was purified by silica gel column chromatography (5% MeOH in DCM) to afford **1** (12 mg, 62%) as a bright red solid. ^{1}H NMR (400 MHz, DMSO-d_6) δ 12.12 (s, 1H), 10.64 (s, 1H), 8.70 (t, *J* = 5.6 Hz, 1H), 8.57 (d, *J* = 8.4 Hz, 2H), 8.23 (s, 1H), 8.11 (d, *J* = 8.4 Hz, 2H), 7.81 (*J* = 7.6 Hz, 1H), 7.44 (s, 1H), 4.10–4.01 (m, 2H), 3.85–3.77(m, 1H), 3.32–3.27 (m, 2H), 3.03–2.96 (m, 1H), 2.85 (dd, *J* = 12.6, 9.8 Hz, 1H), 2.08 (t, *J* = 7.4 Hz, 2H), 1.91–1.87 (m, 1H), 1.81–1.77 (m, 1H), 1.71–1.64 (m, 1H), 1.60–1.49 (m, 4H), 1.44–1.40 (m, 1H), 1.34–1.29 (m, 2H). ^{13}C NMR (101 MHz, DMSO-d_6) δ 171.6, 165.4, 165.2, 158.8, 158.2, 151.0, 150.8, 138.3, 134.1, 128.2, 127.7, 121.0, 102.6, 101.5, 53.5, 49.9, 45.5, 35.4, 30.2, 28.8, 26.1, 25.1, 23.6. ESI-(+)-HRMS $[M+H]^+$ calculated for $C_{26}H_{30}ClN_{10}O_2$: 549.2236; found: 549.2245.

Synthesis of 3

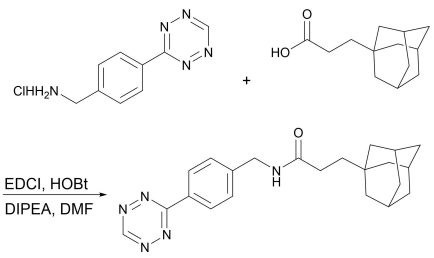

To a solution of 3-(adamant-1-yl)propanoic acid (25 mg, 0.12 mmol, 1.2 equiv.) in DMF (2 mL) was added EDCI (38 mg, 0.20 mmol, 2.0 equiv.), HOBt (4.0 mg, 0.03 mmol, 0.3 equiv.), DIPEA (70 μL, 0.40 mmol, 4.0 equiv.) and (4-(1,2,4,5-tetrazin-3-yl)phenyl)methanamine hydrochloride (18 mg, 0.10 mmol, 1.0 equiv.). The reaction mixture was then stirred at room temperature. After 12 hours, TLC indicated full conversion. The reaction mixture was diluted with water (10 mL) and extracted with EtOAc (3×100 mL). The organic layers were combined, washed with brine, dried over Na_2SO_4, filtered, and concentrated. The crude mixture was purified by silica gel column chromatography (30% EtOAc in petroleum ethers) to give **3** (27 mg, 0.07 mmol, 71%). ^{1}H NMR (400 MHz, $CDCl_3$) δ 10.21 (s, 1H), 8.59 (d, *J* = 8.4 Hz, 2H), 7.51 (d, *J* = 8.0 Hz, 2H), 5.89 (s, 1H), 4.57 (d, *J* = 6.0 Hz, 2H), 2.26–2.22 (m, 2H), 1.96–1.94 (m, 3H), 1.73–1.68 (m, 3H), 1.63–1.59 (m, 3H), 1.50–1.46 (m, 8H). ^{13}C NMR (151 MHz, $CDCl_3$) δ 174.1, 166.4, 158.0, 144.3, 130.9, 128.8, 128.7, 65.7, 43.4, 42.4, 40.0, 37.2, 32.2, 30.6, 28.7, 19.3. ESI-HRMS $[M+H]^+$ calculated for $C_{22}H_{28}N_5O$: 378.2288; found, 378.2287.

Synthesis of 4

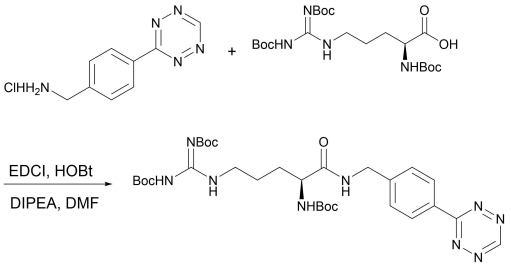

To a solution of Arg-$(Boc)_3$-OH (40 mg, 0.08 mmol, 1.2 equiv.)[29] in DMF (2 mL) was added EDCI (27 mg, 0.14 mmol, 2.0 equiv.), HOBt (1.4 mg, 0.11 mmol, 1.5 equiv.), DIPEA (49 μL, 0.28 mmol, 4.0 equiv.) and (4-(1,2,4,5-tetrazin-3-yl)phenyl)methanamine hydrochloride (13 mg, 0.07 mmol, 1.0 equiv.). The reaction mixture was then stirred at room temperature. After 12 hours, TLC indicated full conversion. The reaction mixture was diluted with water (10 mL) and extracted with EtOAc (3×20 mL). The organic layers were combined, washed with brine, dried over Na_2SO_4, filtered, and concentrated. The residue was purified by silica gel column chromatography (30% EtOAc in petroleum ethers) to give **4** (31 mg, 0.05 mmol, 69%). ^{1}H NMR (400 MHz, $CDCl_3$) δ 11.42 (s, 1H), 10.20 (s, 1H), 8.55 (d, *J* = 8.4 Hz, 2H), 8.43 (s, 1H), 7.47 (d, *J* = 8.0 Hz, 2H), 7.12 (s, 1H), 5.71 (s, 1H), 4.57 (d, *J* = 6.0 Hz, 2H), 4.30 (t, *J* = 6.6 Hz, 1H), 3.50–3.37 (m, 2H), 1.77–1.68 (m, 4H), 1.49 (s, 9H), 1.44 (s, 9H), 1.43 (S, 9H). ^{13}C NMR (101 MHz, $CDCl_3$) δ 172.6, 167.8, 166.4, 163.4, 157.9, 156.7, 156.0, 153.4, 144.0, 132.4, 131.0, 130.7, 129.0, 128.7, 128.3, 83.5, 80.2, 79.6, 65.7, 54.4, 53.6, 40.0, 30.7, 29.1, 28.5, 28.4, 28.2, 26.1, 19.3, 13.8. ESI-HRMS $[M+H]^+$ calculated for $C_{30}H_{45}N_9O_7$: 644.3515; found, 644.3514.

Molecular and Cell Biology Experiments

Cloning

All vectors were generated and propagated using *E. coli* Stbl3 (KT Life Technology, #KTSM110L). Plasmids were isolated from 10 mL cultures using a commercial kit (Omega, #D6943-03). Restriction digestion was conducted with FastDigest restriction enzymes (ThermoFisher). PCR amplification was achieved using PrimeSTAR Max polymerase (Takara, #R045A). DNA fragments were electrophoresed on 1% agarose-TAE gel and visualized using SYBR Safe (Invitrogen, #S33102). Desired bands were excised and extracted using a commercial kit (Omega, #D2500-02). T4 DNA ligase (ThermoFisher, #15224-041) was used for T4 DNA ligation, and NEBuilder HiFi DNA Assembly Master Mix (NEB, #E2621S) was used for Gibson assembly. All yielded constructs were confirmed via Sanger sequencing.

The PKA–Cα-QR (*PRKACA*) and UBE2L3 encoding plasmids were derived from our previous studies. Genes *Stub1*, *Hsp70A1A*, *UBE2L6*, *UBE2B*, *UBE2C*, *UBE2D1*, *UBE2I*, *UBE2K* and *UBE2S* were subcloned from CCSB hORFeome v5.1 cDNA library. gRNA sequences were designed using CHOPCHOP (https://chopchop.cbu.uib.no/) and synthesized by GENERAL BIOL.

Cell Culture and Transient Transfection

HEK293T cells (National Collection of Authenticated Cell Cultures, #GNHu17) were maintained in DMEM medium supplemented with 10% fetal bovine serum (FBS, TransGen Biotech, #FS401-02) and 1% penicillin and streptomycin (P/S, Gibco, #15140122). Cells were incubated in a humidified atmosphere of 5% (v/v) CO_2 at 37 °C.

For transient transfection, plates were pretreated with 0.1 mg/mL poly-L-lysine (Sangon, #E607015) in sterile water and washed with PBS (Meilunbio, #PWL050). Cells were seeded in a 24-well plate at a density of 3×10^6 HEK293T cells per well. After 24 h, transfection was conducted using Lipofectamine 2000 (ThermoFisher, #11668500) following the manufacturer's protocol.

For CYPK incorporation, cells were co-transfected with *Mm*PylRS/$tRNA_{CUA}$ and cultured in the presence of 0.1 mM CYPK for 48 h. Stock solution of CYPK was prepared by dissolving CYPK (SiChem, #SC-8017) in 0.1 N NaOH to the final concentration of 100 mM.

For BCNK and TCOK incorporation, cells were co-transfected with *Mm*PylRS(AF)/$tRNA_{CUA}$ and cultured in the presence of 0.1 mM BCNK or TCOK for 48 h. Stock solution of BCNK and TCOK was prepared by dissolving BCNK (SiChem, #SC-8014) or TCOK (SiChem, #SC-8008) in 0.1 N NaOH to the final concentration of 100 mM.

Western Blot

Briefly, cells were lysed using RIPA (Merck, #R0278) with a protease inhibitor cocktail (Yamei, #GRF101). Equal volumes of the sample were subjected to SDS-PAGE, followed by transferring to nitrocellulose membranes. Membranes were blocked with TBST (Solarbio, #T1081) containing 5% skim-milk for 1 h at room temperature and then overnight at 4 °C with HA mAb (1:1000, ABclonal, #AE008), FLAG mAb (1:1000, Transgen, #HT201-01), β-Actin mAb (1:1000, ABclonal, #AC004), Ubiquitin mAb (1:1000, Cell Signaling Technology, #3936), Stub1 mAb (1:1000, Abcam, #ab134064), Hsp70 mAb (1:1000, Abcam, #ab2787). After three washing steps, membranes were incubated with HRP-conjugated secondary antibodies (1:20000, ABclonal, #AS014 or 1:20000, ABclonal, #AS003) for 1 h at room temperature and visualized on ChampChemiTM580 visualization system.

Genetic Knockout

Two gRNAs were used for each gene. The gRNA sequences are GAAUCGCGAAGAAGAAGCGC and UGCCGCGGAGCGUGAGAGGU for *HSP70A1A* KO, and CAGGUCGAUGCCGAUCGCCG and UGUCUCCGUCGUUGAUCACC for *Stub1* KO. The corresponding DNA sequences of gRNA were subcloned into pX458 encoding Cas9-T2A-GFP, and the generated plasmids were used for HEK293T transfection. 24 h post transfection, cells with moderate GFP fluorescence were sorted, and single clones were allocated to 96 well plates. Two weeks post sorting, gDNA was extracted using QuickExtract DNA Extraction Solution (Lucigen, #QE09050) and amplified using primers specific to the target regions of the gRNA for knockout validation. Antibodies specific to HSP70 as well as CHIP were used for validation.

Tetrazine Treatment of Cells for Protein Degradation

At 48 hours post transfection, cells were washed with PBS and incubated with tetrazine conjugate at 37 °C in a complete culture medium. Afterwards, cells were washed with PBS and lysed with RIPA (Merck, R0278) for western blot analysis.

For pharmacological inhibition of 26S proteasome, cells were pretreated with 10 μM MG-132 (MedChemExpress, #HY-13259) for 2 h or 10 μM bortezomib (MedChemExpress, #HY-13227) for 1 h. For inhibition of lysosomal degradation, cells were pretreated with 10 nM bafilomycin A1 (MedChemExpress, #HY-100558) for 2 h or 5 μM leupeptin (MedChemExpress, #HY-18234) for 2 h. For inhibition of HSP70, cells were pretreated with 10 μM apoptozole (MedChemExpress, #HY-15098) for 16 h. For inhibition of HSP90, cells were pretreated with 500 nM geldanamycin (MedChemExpress, #HY-15230) for 24 h. For inhibition of 19S proteasome, cells were pretreated with 1 μM b-AP15 (MedChemExpress, #HY-13989) for 2 h. For inhibition of E1, cells were pretreated with 40 μM PYR-41 (MedChemExpress, # HY-13296) for 2 h. Inhibitors were maintained in a culture medium throughout the tetrazine treatment at the corresponding concentrations.

Supporting Information Summary

Figure S1. Structure of unnatural amino acids and the adducts after tethering with tetrazine conjugates **1**–**4** used for logP prediction as a measure of lipophilicity; Figure S2: Plots of Δ(AlogP) and Δ(XLOGP3) for the CYPK′ BCNK′, and TCOK′ series; Figure S3: Structure of UBE2L6 (pdb: 1WZW) in sphere or ribbon model; Figure S4: Abundance of UBE2L6 variants with BCNK at position 69, 73, 74, 118, 119 or 122 under different conditions; Table S1: Predicted logP values using different algorithms; Table S2: Pearson correlation coefficients of pairwise logP values from two different algorithms in Table S1; ^{1}H and ^{13}C NMR spectra; and sequence of the expressed proteins.

Acknowledgements

We are grateful to the Shenzhen Bay Laboratory (SZBL) and National Natural Science Foundation of China (22107076 and 22277079) for the financial support. We thank Yuanshan Luo, Luyu Zhou and Liqing Yang for preliminary works related to this project. We appreciate technical assistance from the NMR and Mass Spectrometry Facility at SZBL. Part of this research was undertaken using the supercomputing facilities at Cardiff University operated by Advanced Research Computing at Cardiff (ARCCA) on behalf of the Cardiff Supercomputing Facility and the HPC Wales and Supercomputing Wales (SCW) projects. We acknowledge the support of the latter, which is part-funded by the European Regional Development Fund (ERDF) via the Welsh Government. Y.-L.W. thanks the financial support from the School of Chemistry at Cardiff University.

Conflict of Interests

The authors declare no conflict of interest.

Data Availability Statement

The data that support the findings of this study are available in the supplementary material of this article.

Keywords: Genetic code expansion · Unnatural amino acid · Tetrazine ligation · Targeted protein degradation · Hydrophobic tagging

[1] D. Chirnomas, K. R. Hornberger, C. M. Crews, *Nat. Rev. Clin. Oncol.* **2023**, *20*, 265–278.
[2] a) L. Zhao, J. Zhao, K. H. Zhong, A. P. Tong, D. Jia, *Signal Transduct Target Ther.* **2022**, *7*, 113; b) Y. Ding, D. Xing, Y. Y. Fei, B. X. Lu, *Chem. Soc. Rev.* **2022**, *51*, 8832–8876; c) J. A. Wells, K. Kumru, *Nat. Rev. Drug Discov.* **2024**, *23*, 126–140.
[3] S. L. Schreiber, J. D. Kotz, M. Li, J. Aube, C. P. Austin, J. C. Reed, H. Rosen, E. L. White, L. A. Sklar, C. W. Lindsley, B. R. Alexander, J. A. Bittker, P. A. Clemons, A. de Souza, M. A. Foley, M. Palmer, A. F. Shamji, M. J. Wawer, O. McManus, M. Wu, B. Zou, H. Yu, J. E. Golden, F. J. Schoenen, A. Simeonov, A. Jadhav, M. R. Jackson, A. B. Pinkerton, T. D. Chung, P. R. Griffin, B. F. Cravatt, P. S. Hodder, W. R. Roush, E. Roberts, D. H. Chung, C. B. Jonsson, J. W. Noah, W. E. Severson, S. Ananthan, B. Edwards, T. I. Oprea, P. J. Conn, C. R. Hopkins, M. R. Wood, S. R. Stauffer, K. A. Emmitte, N. I. H. M. L. P. Team, *Cell* **2015**, *161*, 1252–1265.
[4] T. Wu, H. Yoon, Y. Xiong, S. E. Dixon-Clarke, R. P. Nowak, E. S. Fischer, *Nat. Struct. Mol. Biol.* **2020**, *27*, 605–614.
[5] a) K. Nishimura, T. Fukagawa, H. Takisawa, T. Kakimoto, M. Kanemaki, *Nat. Methods* **2009**, *6*, 917–922; b) K. M. Bonger, L. C. Chen, C. W. Liu, T. J. Wandless, *Nat. Chem. Biol.* **2011**, *7*, 531–537; c) H. K. Chung, C. L. Jacobs, Y. W. Huo, J. Yang, S. A. Krumm, R. K. Plemper, R. Y. Tsien, M. Z. Lin, *Nat. Chem. Biol.* **2015**, *11*, 713–720; d) D. L. Buckley, K. Raina, N. Darricarrere, J. Hines, J. L. Gustafson, I. E. Smith, A. H. Miah, J. D. Harling, C. M. Crews, *ACS Chem. Biol.* **2015**, *10*, 1831–1837; e) B. Nabet, J. M. Roberts, D. L. Buckley, J. Paulk, S. Dastjerdi, A. Yang, A. L. Leggett, M. A. Erb, M. A. Lawlor, A. Souza, T. G. Scott, S. Vittori, J. A. Perry, J. Qi, G. E. Winter, K. K. Wong, N. S. Gray, J. E. Bradner, *Nat. Chem. Biol.* **2018**, *14*, 431–441; f) V. Koduri, S. K. McBrayer, E. Liberzon, A. C. Wang, K. J. Briggs, H. Cho, W. G. Kaelin, *Proc. Natl. Acad. Sci. USA* **2019**, *116*, 2539–2544; g) D. R. Liu, *Science* **2024**, *383*, eadk4422.
[6] D. P. Bondeson, Z. Mullin-Bernstein, S. Oliver, T. A. Skipper, T. C. Atack, N. Bick, M. Ching, A. A. Guirguis, J. Kwon, C. Langan, D. Millson, B. R. Paolella, K. Tran, S. J. Wie, F. Vazquez, Z. Tothova, T. R. Golub, W. R. Sellers, A. Ianari, *Nat. Commun.* **2022**, *13*, 5495.
[7] a) J. L. Gustafson, T. K. Neklesa, C. S. Cox, A. G. Roth, D. L. Buckley, H. S. Tae, T. B. Sundberg, D. B. Stagg, J. Hines, D. P. McDonnell, J. D. Norris, C. M. Crews, *Angew. Chem. Int. Ed.* **2015**, *54*, 9659–9662; b) T. Xie, S. M. Lim, K. D. Westover, M. E. Dodge, D. Ercan, S. B. Ficarro, D. Udayakumar, D. Gurbani, H. S. Tae, S. M. Riddle, T. Sim, J. A. Marto, P. A. Jänne, C. M. Crews, N. S. Gray, *Nat. Chem. Biol.* **2014**, *10*, 1006–1012; c) T. K. Neklesa, D. J. Noblin, A. Kuzin, S. Lew, J. Seetharaman, T. B. Acton, G. Kornhaber, R. Xiao, G. T. Montelione, L. Tong, C. M. Crews, *ACS Chem. Biol.* **2013**, *8*, 2293–2300; d) H. S. Tae, T. B. Sundberg, T. K. Neklesa, D. J. Noblin, J. L. Gustafson, A. G. Roth, K. Raina, C. M. Crews, *ChemBioChem* **2012**, *13*, 538–541; e) T. K. Neklesa, C. M. Crews, *Nature* **2012**, *487*, 308–309; f) T. K. Neklesa, H. S. Tae, A. R. Schneekloth, M. J. Stulberg, T. W. Corson, T. B. Sundberg, K. Raina, S. A. Holley, C. M. Crews, *Nat. Chem. Biol.* **2011**, *7*, 538–543.
[8] a) M. J. C. Long, D. R. Gollapalli, L. Hedstrom, *Chem. Biol.* **2012**, *19*, 629–637; b) Y. Shi, M. J. C. Long, M. M. Rosenberg, S. Li, A. Kobjack, P. Lessans, R. T. Coffey, L. Hedstrom, *ACS Chem. Biol.* **2016**, *11*, 3328–3337.
[9] Y. Asawa, K. Nishida, K. Kawai, K. Domae, H. S. Ban, A. Kitazaki, H. Asami, J. Y. Kohno, S. Okada, H. Tokuma, D. Sakano, S. Kume, M. Tanaka, H. Nakamura, *Bioconjugate Chem.* **2021**, *32*, 2377–2385.
[10] A. Go, J. W. Jang, W. Lee, J. D. Ha, H. J. Kim, H. J. Nam, *Eur. J. Med. Chem.* **2020**, *204*, 112635.
[11] S. W. Xie, F. Y. Zhan, J. J. Zhu, Y. Sun, H. J. Zhu, J. Liu, J. Chen, Z. Y. Zhu, D. H. Yang, Z. S. Chen, H. Yao, J. Y. Xu, S. T. Xu, *Angew. Chem. Int. Ed.* **2023**, *62*, e202217246.
[12] M. Hachisu, A. Seko, S. Daikoku, Y. Takeda, M. Sakono, Y. Ito, *ChemBioChem* **2016**, *17*, 300–303.
[13] a) T. Liu, *J. Mol. Biol.* **2022**, *434*, 167565; b) D. de la Torre, J. W. Chin, *Nat. Rev. Genet.* **2021**, *22*, 169–184; c) A. R. Nödling, L. A. Spear, T. L. Williams, L. Y. P. Luk, Y.-H. Tsai, *Essays Biochem.* **2019**, *63*, 237–266.
[14] I. Nikic, T. Plass, O. Schraidt, J. Szymanski, J. A. Briggs, C. Schultz, E. A. Lemke, *Angew. Chem. Int. Ed.* **2014**, *53*, 2245–2249.
[15] a) Y.-H. Tsai, S. Essig, J. J. James, K. Lang, J. W. Chin, *Nat. Chem.* **2015**, *7*, 554–561; b) J. Cheng, Y. Huang, W.-B. Gan, Y.-H. Tsai, in *Genetically Incorporated Non-Canonical Amino Acids* (Eds.: Y.-H. Tsai, S. J. Elsässer), Humana, New York, NY, **2023**, pp. 215–232.
[16] K. D. Freeman-Cook, C. Autry, G. Borzillo, D. Gordon, E. Barbacci-Tobin, V. Bernardo, D. Briere, T. Clark, M. Corbett, J. Jakubczak, S. Kakar, E. Knauth, B. Lippa, M. J. Luzzio, M. Mansour, G. Martinelli, M. Marx, K. Nelson, J. Pandit, F. Rajamohan, S. Robinson, C. Subramanyam, L. Q. Wei, M. Wythes, J. Morris, *J. Med. Chem.* **2010**, *53*, 4615–4622.
[17] L. A. Spear, Y. Huang, J. H. Chen, A. R. Nodling, S. Virdee, Y.-H. Tsai, *J. Mol. Biol.* **2022**, *434*, 167524.
[18] a) S. W. Xie, J. J. Zhu, J. D. Li, F. Y. Zhan, H. Yao, J. Y. Xu, S. T. Xu, *J. Med. Chem.* **2023**, *66*, 10917–10933; b) Q. D. He, X. F. Zhao, D. L. Wu, S. M. Jia, C. L. Liu, Z. T. Cheng, F. Huang, Y. D. Chen, T. Lu, S. Lu, *Eur. J. Med. Chem.* **2023**, *260*, 115741.
[19] a) A. V. Marenich, C. J. Cramer, D. G. Truhlar, *J. Phys. Chem. B* **2009**, *113*, 6378–6396; b) F. Neese, *Wires Comput Mol Sci* **2022**, *12*, e1606; c) M. D. Hanwell, D. E. Curtis, D. C. Lonie, T. Vandermeersch, E. Zurek, G. R. Hutchison, *J. Cheminformatics* **2012**, *4*, 17; d) R. Mannhold, G. I. Poda, C. Ostermann, I. V. Tetko, *J. Pharm. Sci.* **2009**, *98*, 861–893; e) I. V. Tetko, V. Y. Tanchuk, *J. Chem. Inf. Comput. Sci.* **2002**, *42*, 1136–1145; f) T. J. Cheng, Y. Zhao, X. Li, F. Lin, Y. Xu, X. L. Zhang, Y. Li, R. X. Wang, L. H. Lai, *J Chem Inf Model* **2007**, *47*, 2140–2148; g) S. A. Wildman, G. M. Crippen, *J. Chem. Inf. Comput. Sci.* **1999**, *39*, 868–873.
[20] J. H. Qiu, X. F. Bai, W. J. Zhang, M. X. Ma, W. Y. Wang, Y. Liang, H. B. Wang, J. W. Tian, P. F. Yu, *Front. Pharmacol.* **2022**, *13*, 853993.
[21] C. Cecchini, S. Pannilunghi, S. Tardy, L. Scapozza, *Front. Chem.* **2021**, *9*, 672267.
[22] Y. Wang, J. Zhang, J. Deng, C. Wang, L. Fang, Y. Zhang, J. Li, *CCS Chemistry* **2023**, *5*, 2207–2214.
[23] S. K. Ko, J. Kim, D. C. Na, S. Park, S. H. Park, J. Y. Hyun, K. H. Baek, N. D. Kim, N. K. Kim, Y. N. Park, K. Song, I. Shin, *Chem. Biol.* **2015**, *22*, 391–403.
[24] H. R. Kim, H. S. Kang, H. D. Dim, *IUBMB Life* **1999**, *48*, 429–433.
[25] Y. Saeki, *J. Biochem.* **2017**, *161*, 113–124.
[26] I. Sahu, S. M. Mali, P. Sulkshane, C. Xu, A. Rozenberg, R. Morag, M. P. Sahoo, S. K. Singh, Z. Y. Ding, Y. F. Wang, S. Day, Y. Cong, O. Kleifeld, A. Brik, M. H. Glickman, *Nat. Commun.* **2021**, *12*, 6173.
[27] a) B. Fabre, T. Lambour, L. Garrigues, M. Ducoux-Petit, F. Amalric, B. Monsarrat, O. Burlet-Schiltz, M. P. Bousquet-Dubouch, *J. Proteome Res.* **2014**, *13*, 3027–3037; b) K. B. Hendil, F. Kriegenburg, K. Tanaka, S. Murata, A. M. B. Lauridsen, A. H. Johnsen, R. Hartmann-Petersen, *J. Mol. Biol.* **2009**, *394*, 320–328; c) N. Livnat-Levanon, E. Kevei, O. Kleifeld, D. Krutauz, A. Segref, T. Rinaldi, Z. Erpapazoglou, M. Cohen, N. Reis, T. Hoppe, M. H. Glickman, *Cell Rep.* **2014**, *7*, 1371–1380.
[28] Y. Y. Qu, F. X. Sauvage, G. Clavier, F. Miomandre, P. Audebert, *Angew. Chem. Int. Edit.* **2018**, *57*, 12057–12061.
[29] H. Y. Mi, J. L. Liu, M. M. Guan, Q. W. Liu, Z. Q. Zhang, G. D. Feng, *Talanta* **2018**, *187*, 314–320.

Manuscript received: July 15, 2024
Accepted manuscript online: September 2, 2024
Version of record online: ■■, ■■

RESEARCH ARTICLE

In this study, we demonstrate that genetically incorporated unnatural amino acids containing strained alkene or alkyne groups can serve as minimalist tags for targeted protein degradation. Specifically, we observed the degradation of kinases and E2 ubiquitin-conjugating enzymes with strained alkene or alkyne functionalities upon treatment with hydrophobic tetrazine conjugates.

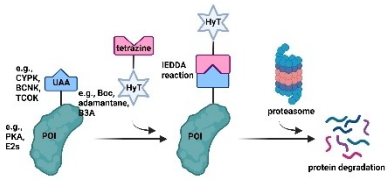

J. Chen, G. Dai, S. Duan, Y. Huang, Y.-L. Wu, Z. Xie*, Y.-H. Tsai**

1 – 10

Selective Protein Degradation through Tetrazine Ligation of Genetically Incorporated Unnatural Amino Acids